Coordinated Integration of Distributed Energy Resources in Unit Commitment

Usman Munawar , Zhanle Wang

Electronic Systems Engineering, University of Regina, Regina, SK, Canada, S4S 0A2

Abstract

Distributed energy resources, such as electric vehicles and roof-top solar panels have become increasingly popular and essential components of power distribution systems. However, their growth poses significant challenges to system operation, such as bidirectional power flow, intermittent power generation, increased peak demand, and unexpected frequency/voltage fluctuation. To tackle these challenges, we developed a vehicle-to-grid model, which incorporated dynamic electric vehicles usages, such as driving times, driving distance, and charging/discharging locations. The machine learning method of principal component analysis and XGBoost were used to develop the solar energy prediction model. We also developed a novel unit commitment model to coordinate and aggregate the distributed energy resources in power generation economic dispatch. Electric vehicle charging was used as elastic demand and electric vehicle discharging was used as power generation sources. The solar energy was considered as a negative load. Simulation results showed that uncontrolled electric vehicle charging and solar energy could negatively impact the power systems. For example, the load ramping rate was increased by 384%. Simulation results also showed that the proposed models could mitigate the negative impact and improve energy efficiency. For example, the peak demand, load ramping rate and average generation cost were reduced by 21%, 79%, and 27%.

Keywords: distributed energy resources, unit commitment, solar energy, electric vehicle, vehicle to grid, demand response.

Nomenclature

Sets

$\mathcal{I}$	The set of EVs
$\mathcal{J}$	The set of power generation units
$\mathcal{T}$	Time horizon

Greek

α^j, β^i	Constant coefficients

Symbols and Variables

Δt	Time interval
$\overline{P_l^{\mathrm{EV}}}$	Rated EV charging/discharging power
$\overline{p_t^j}$	Maximum power generation limit of the unit j
SOC_0	Initial SOC
$\mathrm{SOC}_{\max}$	Maximum SOC
$\mathrm{SOC}_{\max}$	Minimum SOC
$\mathrm{SOC}_{\mathrm{acc}}$	Accepted SOC level at driving times
$\underline{p_t^j}$	Minimum power generation limit of the unit j
$\underline{t_{\mathrm{off}}}$	Minimum down time
$\underline{t_{\mathrm{on}}}$	Minimum up time
$B_t^{\mathrm{EV}^i_{\downarrow}}$	Binary variables indicating EV discharging status
$B_t^{\mathrm{EV}^i_{\rightarrow}}$	Binary variables indicating EV driving status
$B_t^{\mathrm{EV}^i_{\uparrow}}$	Binary variables indicating EV charging status
$c_i(\cdot)$	Discharging cost of an EV

$c_j(\cdot)$	Operation cost of a generation unit
C_t^{A}	Actual generation cost
C_t^{M}	Generation cost in an electricity market
i, j, k	Index
p_t^j	Amount of power generation
$p_t^{\mathrm{EV}_\downarrow^i}$	EV discharging power
$p_t^{\mathrm{EV}_\rightarrow^i}$	EV driving power
$p_t^{\mathrm{EV}_\uparrow^i}$	EV charging power
$p_t^{\mathrm{EV}^i}$	Power consumption of the i^{th} EV at time slot t
$P_{\mathrm{Dri}}^{\mathrm{EV}}$	Rated EV driving power
R_j^{D}	Ramping down limit
R_j^{U}	Ramping up limit
t	Time
$t_{i,1}, t_{i,3}$	Departure times of the i^{th} EV
$t_{i,2}, t_{i,4}$	Arrival times of the i^{th} EV
y_j^t	On/off status of unit j at time t
AT	Ambient Temperature
PA	Panel Area
PE	Panel Efficiency
R	Radiation Value
SPG	Solar Power Generation

Acronyms

CCG	Combined-Cycle Gas
DER	Distributed Energy Resources
DR	Demand Response
EV	Electric Vehicle
PCA	Principal Component Analysis
SCG	Simple-Cycle Gas
SOC	State of Charge
UC	Unit Commitment
V2G	Vehicle-to-Grid
XGBoost	Extreme Gradient Boosting

1. Introduction

The worldwide power system transition from the conventional grid to smart grid paradigm is promoting the integration of distributed energy resources such as roof-top solar, small-scale wind turbines, electrical energy storage systems, electric vehicles (EV), and demand response (DR) [1]. However, the growth of distributed energy resources (DER) poses significant challenges to the power system operation and control, such as bidirectional power flow, intermittent power generation, increased peak demand, and unexpected frequency/voltage fluctuation [2]. Therefore, DER aggregators and grid operators need to prepare for high-level distributed energy resource penetration to the power system.

Solar and wind energy are intermittent and not economic dispatchable; therefore, accurate short-term forecasting is paramount for their integration. Among other methods such as physical and statistical models, the machine learning method becomes increasingly suitable for short-term renewable energy forecasting [3, 4]. However, the appropriate selection of machine learning models and data features remains a significant challenge. A framework to evaluate various machine learning models and feature selection methods was developed in [5], and the best combination to forecast short-term solar power was discovered.

Besides accurate forecasting, energy storage systems are also helpful in renewable energy integration into power systems because energy storage can absorb the uncertainty of renewable energy. However, large-scale economic energy storage is not mature yet [6, 7]. Alternatively, as EVs have significant batteries, they can be considered as mobile energy storage with time-varying parameters such as driving distance/period and charging/discharging locations [8]. However, uncontrolled EV charging can significantly increase peak demand [9].

To mitigate the challenge of renewable energy and EV integration, they must be included in the power system operation routine, e.g., unit commitment (UC) that economically dispatches power generation to meet demand [10, 11]. Power system flexibility metrics, e.g., the ramping rate of a load profile, were proposed to assess the flexibility of the power system for renewable energy integration [12]. Energy storage and combined heat & power generation were used in a UC model to compensate the intermittent solar energy [13].

Concentrating solar power technology could also smooth out the variation of solar energy because it could store energy [14]. The uncertainty in UC model was reviewed in [15]. The security constrained UC model considering the uncertainty of wind generation was developed in [16]. Alternatively, stochastic UC models were developed to cope with the uncertainty from high level penetration of the solar energy [17, 18]. These UC models focused on coping with the uncertainty of solar energy, and the solar energy information was from actual data or predicted by other sources.However, accurate solar prediction models were not integrated into the UC models.

EVs are parked 95% of the time on average, and EVs can be controlled to charge or discharge during the parking time, known as the vehicle-to-grid (V2G) application [19]. V2G can be incorporated into UC models. For example, a V2G model was developed to analyze the impact of bidirectional flow capacity on power generation dispatch [20]. The EV discharging capacity was used as the spinning reserve in a UC model to absorb the uncertainty from renewable energy [21]. Both the EV charging and discharging in a V2G application were coordinated by a UC model to fill the load valley from renewable energy integration [22]. Furthermore, a security constrained UC model was developed to cope with extreme scenarios of uncertainty from renewable energy and EV penetration [23, 24, 25]. However, these models did not consider dynamic EV usages, such as driving times, driving distance, and plugin locations.

UC can be formulated into mixed-integer programming models [26, 27]. Methods have been developed to solve UC models, such as Lagrangian relaxation [28], particle swarm optimization [29, 30, 31] and genetic algorithm [32, 33]. Among others, the mixed-integer linear programming was widely used due to its flexibility, high efficiency, high convergent rate [34, 35, 36, 37, 38, 39, 40].

Nonetheless, highly accurate short-term renewable energy prediction models are needed. Also, the dynamic EV usages, such as driving times, driving distance, and plugin locations, need to be modeled. To our best knowledge, UC models with integrated both highly accurate short-term renewable energy prediction and the EV dynamic usage have not been developed. In this study, we have developed a highly accurate solar energy prediction model and a V2G model with the dynamic EV usage. A UC model was further developed, which incorporated the solar prediction and V2G models.

The contributions of this work are summarized as follows:

1. A V2G model is developed, in which the dynamic EV usages are mod-

eled, such as driving times, driving distance, and charging/discharging locations.

2. A UC model with integrated solar energy prediction and V2G models is developed. This model incorporates EV discharging as power generation and controlled EV charging as elastic demand under DR.
3. The proposed models can be used to integrate a high level penetration of EV and renewable energy to power systems.

The paper is organized as follows. Section II describes the problem formulation and Section III presents case the simulation results. The discussion is given in Section IV and the conclusion is presented in Section V.

2. Problem Formulation

The main objective of this study is to economically and reliably integrate DERs including EVs and solar energy into power systems. Fig. 1 shows the system architecture. DER aggregators collect the information from DERs and aggregate DERs to participate in UC. Solar energy is predicted and considered as a negative load in the system. The V2G model incorporates dynamic EV usage. The predicted EV discharging energy is used as power generation in the UC model for economic dispatch. The predicted EV charging energy is used as elastic demand under DR. Four conventional generators are also used, including coal, combined-cycle gas, simple-cycle gas, and diesel. The developed UC model economically dispatches conventional generation units, EV discharging capacity, and EV charging capacity. The major outcomes include reduced generation cost, lower peak demand, lower load variation, and less greenhouse gas emissions.

This section presents the dynamic EV usage and V2G model, the solar energy prediction model, and the UC model.

2.1. Dynamic EV Usage and V2G

A fleet of EVs can be used as a battery bank for power system operation and control. For instance, EV discharging can be used as distributed energy resources, and controlled EV charging can be used as flexible demand in DR. However, this battery bank has dynamic parameters such as driving times, driving distance, and charging/discharging locations.

Fig. 2 shows the plug-in and dynamic driving times. Blue color presents EV plug-in periods at homes or workplaces while green color shows driving

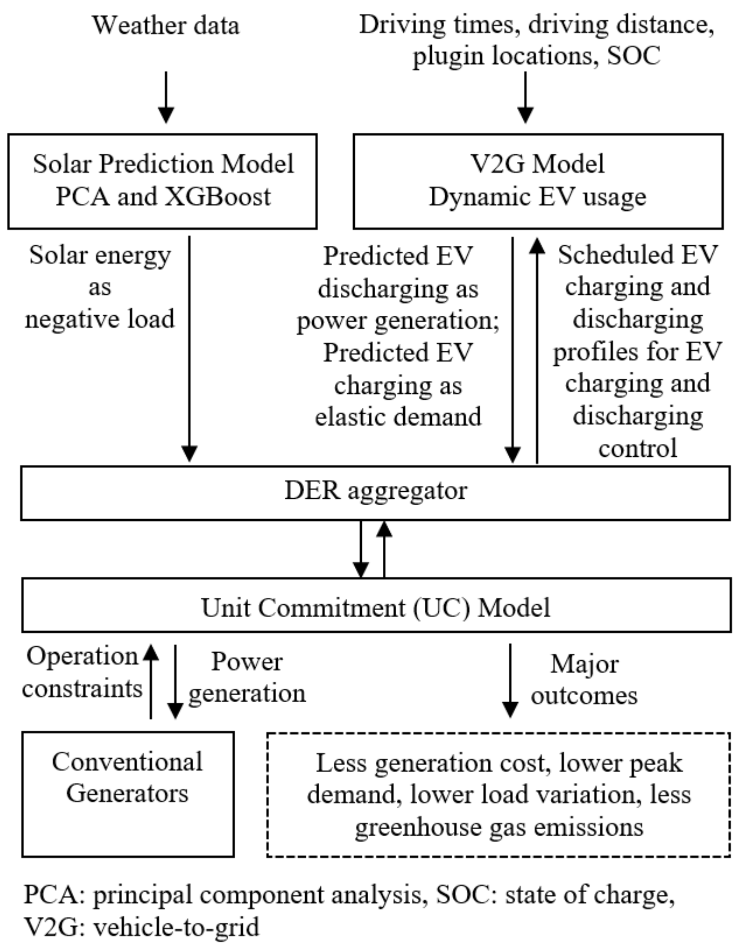

Figure 1: System architecture

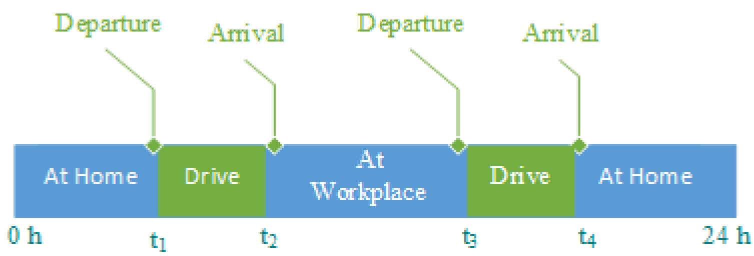

Figure 2: The diagram of important EV usage times

periods. Throughout the day, there are two driving periods from home t_1 to workplace t_2 and from workplace t_3 to home t_4. As the daily routine of the people are similar, the values of t_1, t_2, t_3 and t_4 tends to be normally distributed [8].

The V2G problem is modeled as follows.

$$p_t^{\mathrm{EV}^i} = p_t^{\mathrm{EV}^i_{\uparrow}} - p_t^{\mathrm{EV}^i_{\downarrow}} - p_t^{\mathrm{EV}^i_{\rightarrow}} \tag{1}$$

$$0 \leq p_t^{\mathrm{EV}^i_{\uparrow}} \leq B_t^{\mathrm{EV}^i_{\uparrow}} \overline{P_l^{\mathrm{EV}}}, \forall i, t \in [t_{i,2}, t_{i,3}] \cup [t_{i,4}, t_{i,1}] \tag{2}$$

$$0 \leq p_t^{\mathrm{EV}^i_{\downarrow}} \leq B_t^{\mathrm{EV}^i_{\downarrow}} \overline{P_l^{\mathrm{EV}}}, \forall i, t \in [t_{i,2}, t_{i,3}] \cup [t_{i,4}, t_{i,1}] \tag{3}$$

$$p_t^{\mathrm{EV}^i_{\rightarrow}} = B_t^{\mathrm{EV}^i_{\rightarrow}} P_{\mathrm{Dri}}^{\mathrm{EV}}, \forall i, t \in [t_{i,1}, t_{i,2}] \cup [t_{i,3}, t_{i,4}] \tag{4}$$

$$B_t^{\mathrm{EV}^i_{\uparrow}}, B_t^{\mathrm{EV}^i_{\downarrow}}, B_t^{\mathrm{EV}^i_{\rightarrow}} \in \{0, 1\} \tag{5}$$

$$B_t^{\mathrm{EV}^i_{\uparrow}} + B_t^{\mathrm{EV}^i_{\downarrow}} + B_t^{\mathrm{EV}^i_{\rightarrow}} \leq 1 \tag{6}$$

$$\mathrm{SOC}_{i,ts} = \mathrm{SOC}_0 + \sum_{t=0}^{ts} p_t^{\mathrm{EV}^i} \Delta t, \quad \forall i \tag{7}$$

$$\mathrm{SOC}_{\min} \leq \mathrm{SOC}_{i,ts} \leq \mathrm{SOC}_{\max}, \quad \forall i, t \tag{8}$$

$$\mathrm{SOC}_{i,t_1} \geq \mathrm{SOC}_{\mathrm{acc}}, \quad \forall i \tag{9}$$

$$\mathrm{SOC}_{i,t_3} \geq \mathrm{SOC}_{\mathrm{acc}}, \quad \forall i \tag{10}$$

where $p_t^{\mathrm{EV}^i}$ is the power consumption of the i^{th} EV at time slot t. $p_t^{\mathrm{EV}^i_{\uparrow}}, p_t^{\mathrm{EV}^i_{\downarrow}}$ and $p_t^{\mathrm{EV}^i_{\rightarrow}}$ are the EV power consumption of charging, discharging and driving respectively. $B_t^{\mathrm{EV}^i_{\uparrow}}, B_t^{\mathrm{EV}^i_{\downarrow}}$ and $B_t^{\mathrm{EV}^i_{\rightarrow}}$ are binary variables indicating EV status of charging, discharging and driving respectively. For example, $B_t^{\mathrm{EV}_\uparrow^i} = 1$ indicates EV charging and $B_t^{\mathrm{EV}_\uparrow^i} = 0$ indicates no EV charging.

Eq. (2) shows that the EVs can be charged with the power between 0 and rated charging power when they are at homes or workplaces. $t \in [t_{i,2}, t_{i,3}] \cup [t_{i,4}, t_{i,1}]$ is the time period when the i^{th} EV is at homes or workplaces. This time is different among EVs. Likewise, Eq. (3) shows the EV discharging constraint when they are at homes or workplaces. Eq. (4) is the power consumption during the driving period.

Eq. (5) shows that $B_t^{\mathrm{EV}_\uparrow^i}, B_t^{\mathrm{EV}_\downarrow^i}, B_t^{\mathrm{EV}_\rightarrow^i}$ are binary variables. Eq. (6) shows the EV cannot be charging, discharging and driving simultaneously.

Eq. (7) shows the SOC of the i^{th} EV at t, where Δt is the time duration of each interval. Eq. (8) is a constraint for limiting the individual EV's SOC between the minimum and maximum limit of SOC, e.g., 0% and 100%. Eq. (9) and Eq. (10) constraints the SOC at start of driving times (t_1 and t_3), which indicates that the EV should have sufficient energy for driving.

This V2G model is incorporated into the UC model discussed in Section *2.3*.

2.2. Solar Prediction

Solar energy prediction is paramount in power system operation since solar energy is intermittent and generally non-dispatchable. Machine learning algorithms play an important role in solar energy prediction. Our earlier research in [5] showed that the combination of principal component analysis (PCA) and XGBoost provided the most accurate prediction among others: PCA with random forest, PCA with neural networks, feature importance with XGBoost, feature importance with neural networks, and feature importance with random forest.

Therefore, this study uses PCA and XGBoost for solar energy prediction. Specifically, we use PCA for feature selection and use XGBoost to map the selected features to solar radiation signals. To train the predictive model, we use the weather data in the period of September-December, 2016, from the Kaggle database [41]. The data includes 11 attributes such as date, time, radiation, temperature, etc.

The following steps are carried out [5].

Step 1. Data pre-processing: 1) The data are cleaned. 2) The time and date are extracted from the UNIX time. 3) The sunset and sunrise times are used to extract the length of the daytime. 4) The data are divided into three data sets: training, cross-validation, and test.

Step 2. Manual feature selection: By using statistical methods, the attributes are ordered based on the correlations with solar radiation. The most seven correlated attributes are selected: temperature, humidity, pressure, wind direction, wind speed, day, and time.

Step 3. PCA for feature selection: PCA is used to reduce the seven attributes into four components.

Step 4. XGBoost to map the selected features to solar radiation signals: XGBoost is a machine learning algorithm based on a sequential ensemble of decision trees, where weak learners can learn jointly to build a strong learner.

The training and cross-validation datasets are used to train the parameters and hyperparameters. For example, the number of trees, maximum depth of trees, and step size were tuned as 70, 13, and 0.05, respectively. The final test using the test dataset shows 99.4% accuracy.

Finally, the predicted solar radiation is used to estimate the solar power generation, which is calculated as follows.

$$SPG = PE \cdot PA \cdot R \cdot [1 - 0.005(AT - 25)] \tag{11}$$

where PE is the panel efficiency, and PA is the panel area. R is the radiation value, while AT is the ambient temperature. SPG represents solar power generation.

The predicted solar energy is considered a negative demand and incorporated into the UC model discussed in the next section.

2.3. Unit Commitment Model with V2G and Solar Prediction

UC is used to economically dispatch generation units to meet demand. Unlike a conventional UC model, the proposed model incorporates the V2G model and solar energy prediction. EV discharging is used as power generation units, and EV charging is used as an elastic load under the concept of DR. The predicted solar energy is used as a negative load.

$$\underset{p_t^j, p_t^{\mathrm{EV}_\downarrow^i}, p_t^{\mathrm{EV}_\uparrow^i}}{\text{minimize}} \quad \sum_{t \in \mathcal{T}} \left[\sum_{j \in \mathcal{J}} c_j(p_t^j) + \sum_{i \in \mathcal{I}} c_i(p_t^{\mathrm{EV}_\downarrow^i}) \right] \tag{12}$$

subject to:

$$\sum_{j\in\mathcal{J}} p_t^j + \sum_{i\in\mathcal{I}} p_t^{\mathrm{EV}_\downarrow^i} = p_t^d - p_t^s + \sum_{i\in\mathcal{I}} p_t^{\mathrm{EV}_\uparrow^i},\ \forall t\in\mathcal{T} \tag{13}$$

$$y_t^j \in \{0,1\}, \quad \forall t\in\mathcal{T}, j\in\mathcal{J} \tag{14}$$

$$\underline{p_t^j} y_t^j \le p_t^j \le \overline{p_t^j} y_t^j, \quad \forall t\in\mathcal{T}, j\in\mathcal{J} \tag{15}$$

$$R_j^{\mathrm{U}} \le p_j^t - p_j^{t-1} \le R_j^{\mathrm{D}}, \quad \forall t\in\mathcal{T}, j\in\mathcal{J} \tag{16}$$

$$\begin{aligned} y_t^j - y_{t-1}^j \le y_k^j \quad & \forall j\in\mathcal{J}, t\in\{2\ldots|\mathcal{T}|-1\}, \\ & k \in \left\{\min\left(t+\underline{t_{\mathrm{on}}}-1, |\mathcal{T}|\right)\right\} \end{aligned} \tag{17}$$

$$\begin{aligned} y_{t-1}^j - y_t^j \le 1 - y_k^j \quad & \forall j\in\mathcal{J}, t\in\{2\ldots|\mathcal{T}|-1\}, \\ & k \in \left\{\min\left(t+\underline{t_{\mathrm{off}}}-1, |\mathcal{T}|\right)\right\} \end{aligned} \tag{18}$$

Eq. (1) - (10)

The objective function is to minimize the generation cost. $\mathcal{T}$ is the set of EV plug-in times. $\mathcal{J}$ is the set of power generation units. p_t^j and $c_j(\cdot)$ is the power generation and cost of the j^{th} power unit, which is defined as follows:

$$c_j(p_t^j) = \alpha^j p_t^j \tag{19}$$

where α^j is constant.

$\mathcal{I}$ is the set of EVs. $c_i(\cdot)$ is the discharging cost of the i^{th} EV, which can be defined as follows.

$$c_i(p_t^{\mathrm{EV}_\downarrow^i}) = \beta^i p_t^{\mathrm{EV}_\downarrow^i} \tag{20}$$

where β^i is constant.

The decision variables include $p_t^j, p_t^{\mathrm{EV}_\downarrow^i}$ and $p_t^{\mathrm{EV}_\uparrow^i}$. Although EV charging ($p_t^{\mathrm{EV}_\uparrow^i}$) is not in the objective function, it is flexible load under DR shown in Eq. (13).

Eq. (13) is the power balance constraint between power generation and demand. p_t^d is a reference load at time t. We define the reference load as the load profile without EV and solar energy penetration. p_t^s represents the solar power at time t. The power are from the power generation units (p_t^j) and EV discharging. The demand includes the net load ($p_t^d - p_t^s$) and the flexible EV charging load.

In Eq. (14) y_j^t is a binary variable, which is the on/off status of unit j at time t. In Eq. (15), $\overline{p_t^j}$ represents the maximum power generation limit of the unit j and $\underline{p_t^j}$ is the minimum power generation that the unit j needs to produce once it is on due to physical constraints. Eq. (16) exhibits the ramping up/down constraint of the unit j, where R_j^{U} and R_j^{D} show ramping up and down limit respectively.

Eq. (17) is the minimum on-time constraint, which means that the power generation unit has to remain on for a minimum time $\underline{t_{\mathrm{on}}}$ after it is switched on due to economical reasons or mechanical design limits. Similarly, as observed in Eq. (18), a unit has to remain off for a minimum time $\underline{t_{\mathrm{off}}}$ after it is switched off. $|\mathcal{T}|$ is the cardinality of the set $\mathcal{T}$.

3. Simulation Results and Analysis

To evaluate the proposed models, cases studies were conducted in 3 scenarios:

1. Reference scenario: no EV nor solar energy penetration
2. Uncontrolled EV and solar energy penetration
3. V2G and solar energy penetration with 30% EVs penetration
4. V2G and solar enegry penetration with 80% EVs penetration

3.1. Experimental Setup

This study simulated a power system having 300 homes. We first determined the energy consumption of the simulated power system as follows. The electricity usage can be grouped as residential, industrial, and commercial sectors, while the residential sector consumes 1/3 of total electricity [42, 43]. Furthermore, the average electricity usage per household is 30 kWh/day [44]. Therefore, the energy consumption of the simulated power system was calculated as $0.03\,\mathrm{MWh} \times 300 \times 3 = 30\,\mathrm{MWh}$. The load profile from PJM [45] was used and scaled down to fit the magnitude of our simulation. Fig. 3 shows the scaled load profile, and we denote it as the reference load profile in this study.

Table 1 summarizes the parameters for the V2G model. We assumed that 30% of the consumers have EVs; therefore, 90 EVs were considered. The start EV driving times follow a normal distribution, and the expected value μ and the standard deviation σ are shown in the table. The driving time period was assumed as 45 minutes [8]; therefore $t_2 = t_1 + 45$ and $t_4 = t_3 + 45$. The

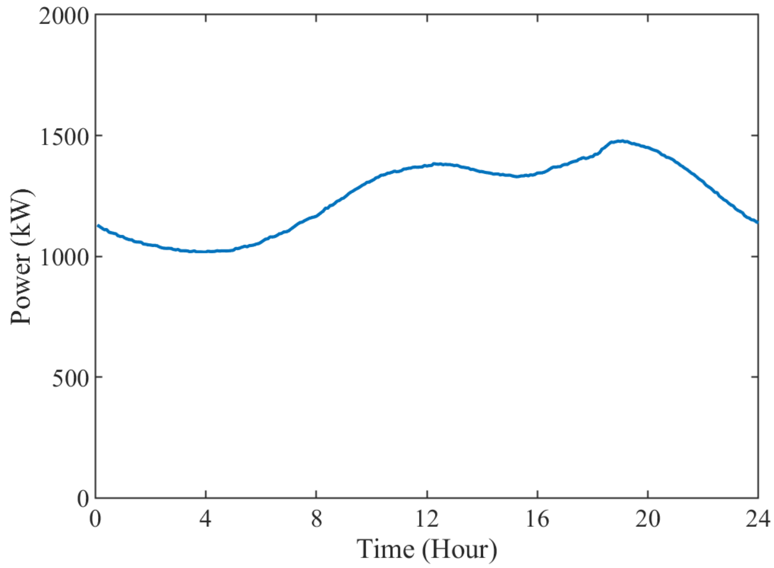

Figure 3: The reference load profile (Scaled from the actual load profile on October 27, 2019 from PJM. [45])

rated power ($\overline{P_l^{\mathrm{EV}}}$) of EV charging/discharging was 3.3 kW at both home and workplace. The rated power for EV driving ($P_{\mathrm{Dri}}^{\mathrm{EV}}$) was 8 kW. In addition, the EV battery capacity was 50 kWh, and the initial SOC was 50%. The maximum and minimum SOC were 0% and 100%.

The solar model discussed in Section II.B was used to predict the solar energy based on the weather data in [41]. We assumed that 20% of homes have roof-top solar, and 10 kW PV system was designed with overall 70% system efficiency. The total PV area per home roof-top was 87 m^2 with PV panel efficiency of 16%. Eq. 11 was used to calculate the solar power generation. Table 2 shows the parameters. Fig. 4 shows the predicted solar power.

Table 3 summarizes the parameters of the UC model for conventional power generation units: coal ($j = 1$), combined-cycle gas ($j = 2$), simple-cycle gas ($j = 3$) and diesel ($j = 4$). The combined-cycle gas units use both gas-turbine and heat recovery steam-turbine and therefore are more efficient than simple-cycle gas units. However, simple-cycle gas units have the advantages of quick start and high ramping rate.

We also considered the power generation dispatch in an electricity mar-

Table 1: Major Parameters for V2G Model

Parameter	Values
$\beta^i, \forall i \in \mathcal{J}$	\$50/MWh
t_1 (normal distribution)	$\mu = 7:00$ and σ= 1 hour [8, 9]
t_3 (normal distribution)	$\mu = 17:00$ and σ= 2.8 hours [8, 9]
$\mathcal{T}$	24 hours
Time Interval	5 minutes
$\overline{P_l^{\mathrm{EV}}}$	3.3 kW [8]
$P_{\mathrm{Dri}}^{\mathrm{EV}}$	8 kW
$\mathrm{SOC}_{\mathrm{min}}$	0%
$\mathrm{SOC}_{\mathrm{max}}$	100%
$\mathrm{SOC}_{\mathrm{acc}}$	50%

Table 2: Parameters for Solar Prediction

Parameter	Values
Rated Solar Power per home	10 kW
Ambient Temperature	28 C^o
PV Efficiency (PE)	16%
System Efficiency	70%
PV Area (PA)	87 m^2

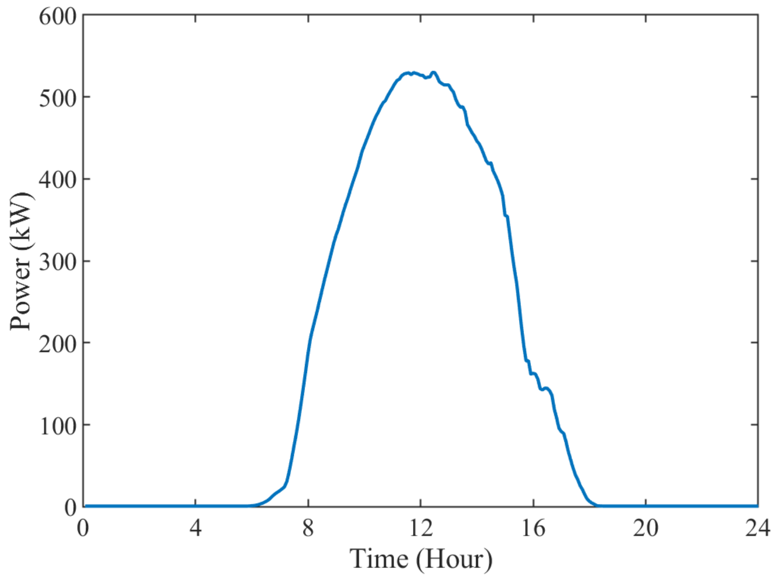

Figure 4: Predicted solar power

ket. The electricity market is cleared when the power generation units are dispatched to meet the demand. All the dispatched generation units are paid the same as the generation unit with the highest generation cost. The market-based generation cost was calculated as follows.

$$C_t^{\mathrm{M}} = \max\left[c_j(p_t^j)\right] \tag{21}$$

The proposed optimization models were solved by the CVX with the Gurobi solver [46, 47, 48].

3.2. Scenario #1: Reference Scenario

The reference scenario did not consider the integration of solar energy and EVs. The UC model without V2G was solved to dispatch the four power units.

Fig. 5 shows the economic dispatch of the four power generation units, where the area plots show the power production of the units, and the envelope shows the total generation. The generation must always meet the demand. The energy consumption was 30 MWh. The total generation cost was \$1538. The average generation cost was $1538/30 = \$51.3$/MWh.

Table 3: Major Parameters of the UC Model

Parameter	Coal	CCG	SCG	Diesel
α^j (\$/MWh)	28.1	30.2	45	62
$\overline{p_t^j}$ (kW)	750	400	400	1000
$\underline{p_t^j}$ (kW)	10	4	2	0
$\underline{t_{\text{on}}}$ (minutes)	30	10	20	5
$\underline{t_{\text{off}}}$ (minutes)	15	10	20	5
R_j^{U} (kWh/5-min)	0.5	2	4	100
R_j^{D} (kWh/5-min)	-0.5	-2	-4	-100

CCG: Combined-Cycle Gas. **SCG:** Simple-Cycle Gas

The peak demand and the variance of the reference load were 1478.1 kW and 22237.0 kW, respectively. The maximum ramping rate was 13.9 kWh/5-min.

3.3. Scenario #2: Uncontrolled EV and solar energy penetration

To evaluate the impact of uncontrolled EV charging and solar energy penetration on the power system, three sub-scenarios were designed: #2A - uncontrolled EV charging penetration, #2B - solar energy penetration, and #2C - both uncontrolled EV charging and solar energy penetration.

The blue line in Fig. 6 shows the load profile in Scenario #2A. The peak demand and the variance of the load profile were 1741.7 kW and 42939.0 kW, respectively. The maximum ramping rate 67.3 kWh/5-min. The energy consumption was 32 MWh. The generation cost was \$1698. The average generation cost was \$53.1/MWh.

The red line in Fig. 6 shows the net load profile in the case of solar energy penetration. The predicted solar power is shown in Fig. 4 acts as a negative load. The peak demand and the variance of the load profile were 1477.4 kW and 37529.0 kW, respectively. The energy consumption was 26.4 MWh. The generation cost was \$1398. The average generation cost was \$52.9/MWh

Fig. 7 shows the reference load profile and the net load profile with both uncontrolled EV and solar penetration. With both uncontrolled EV and solar penetration, the peak demand and the variance of the load profile were 1741.0 kW and 82699.0 kW, respectively. The energy consumption was 28.4 MWh. The generation cost was \$1554. The average generation cost was \$54.9/MWh.

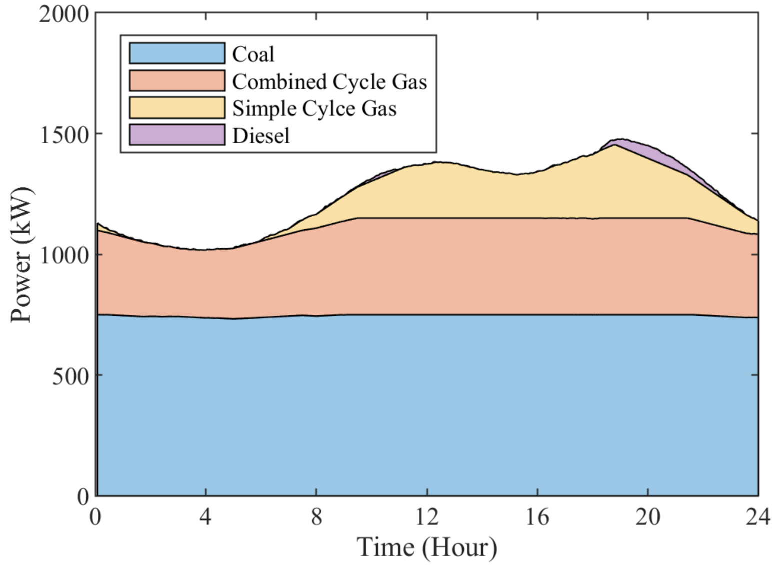

Figure 5: Power generation of different units in Scenario #1

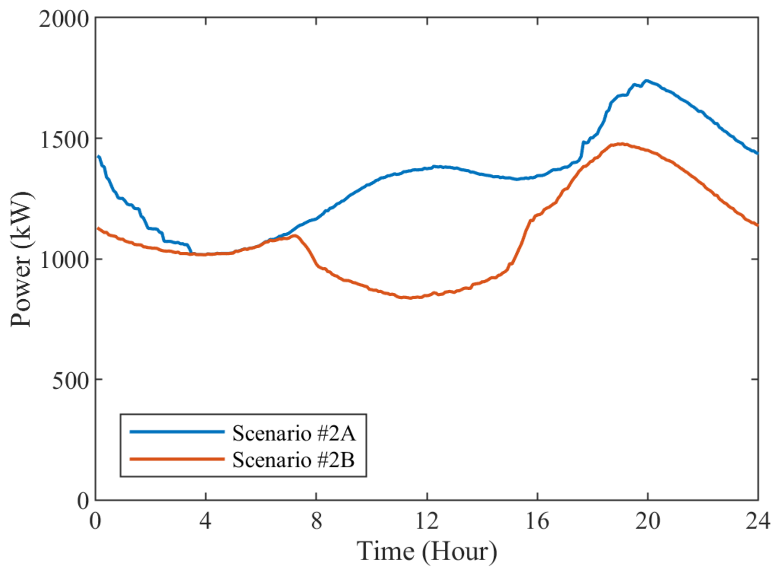

Figure 6: Load profiles of Scenario #2A and #2B

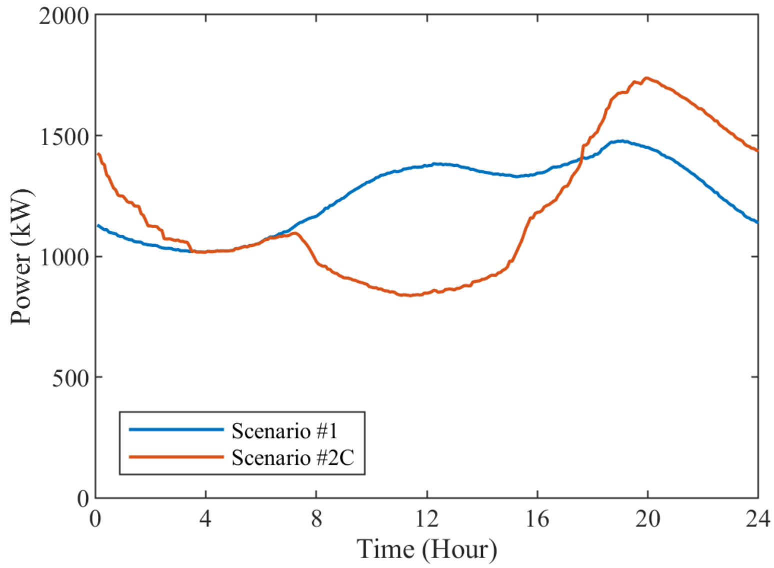

Figure 7: Load profiles of Scenario #1 and #2C

Fig. 8 shows the economic dispatch of the four power generation units for Sub-scenario #2C.

The intermittent solar energy can significantly increase the net load ramping rate, which can pose a significant challenge for power system operation. The maximum ramping rate was 67 kWh/5-min for Scenario #2B and #2C. The ramping rate was increased by 384% compared with Scenario #1.

3.4. Scenario #3: V2G and solar energy penetration

In this scenario, the UC model with V2G was applied in the case with both EV and solar penetration. EV charging was included as flexible demand and EV discharging was included as power generation in the UC model. Eq. 20 was used to calculate the EV discharging cost.

Fig. 9 shows the load profiles of Scenario #2C and #3. As can be seen, the peak demand was reduced from 1741.0 kW to 1376.6 kW and the variance of the load profile was reduced from 82699.0 to 16808.0 kW. The maximum ramping rate was reduced from 67.4 kWh/5-min to 14.1 kWh/5-min. Fig. 10 shows uncontrolled EV charging and the EV charging and discharging curves under V2G. Blue line shows the uncontrolled EV charging as the reference. Red line shows the aggregated EV charging/discharging curves under V2G,

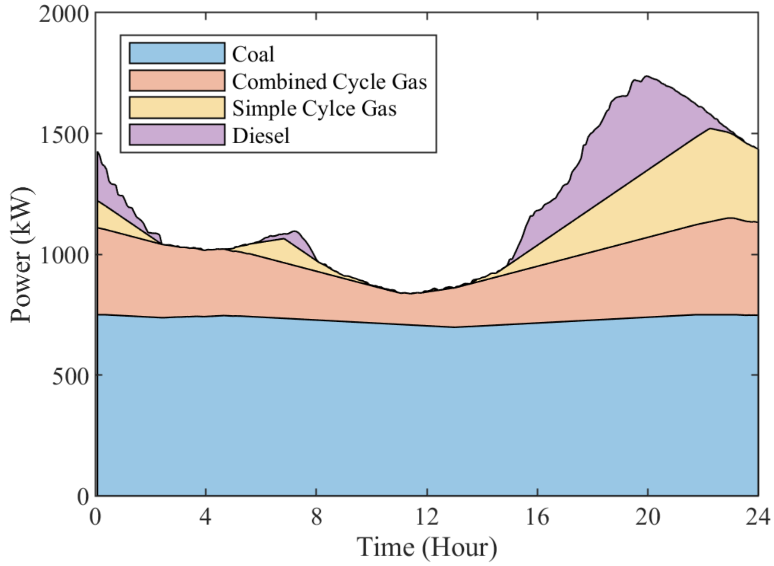

Figure 8: Power generation of different units in Scenario #2C

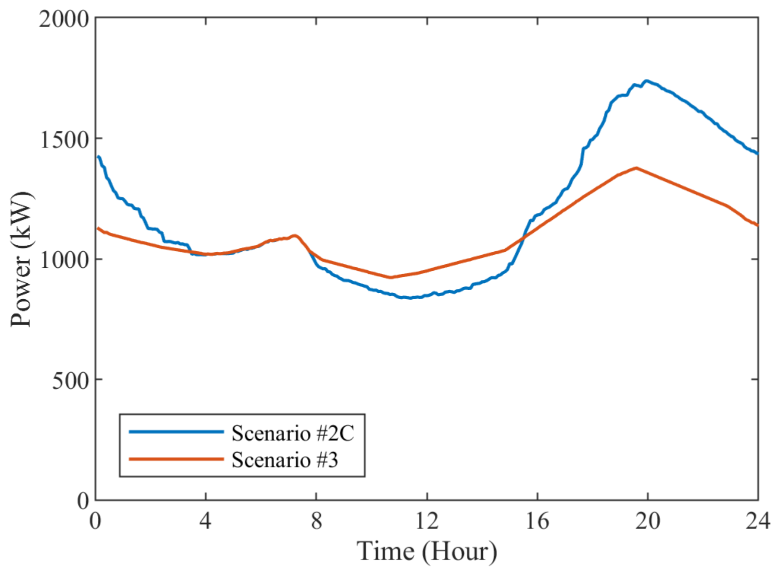

Figure 9: Load profiles of Scenario #2C and #3

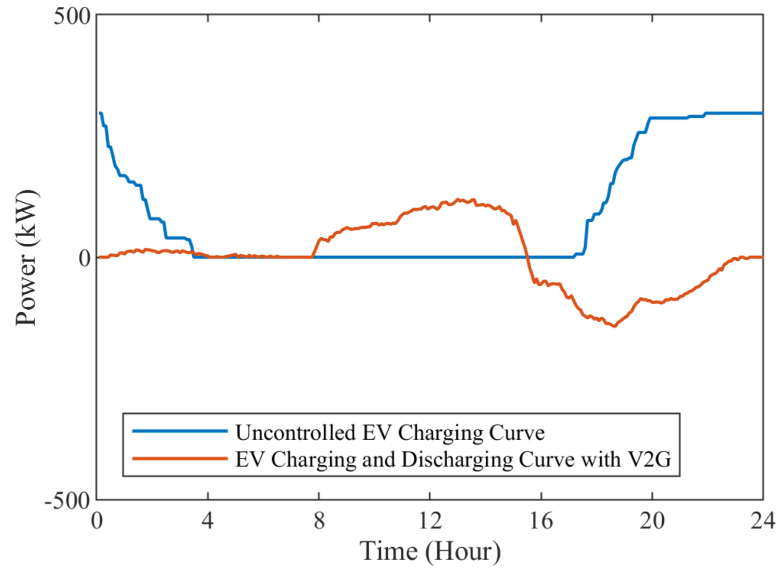

Figure 10: Uncontrolled EV charging curve (Scenario #2C) and EV charging and discharging curve with V2G (Scenario #3)

where positive values were EV charging and negative values were EV discharging. As can be seen, the EVs were under charging during the load valley period. This is the period when there is plenty of solar energy available. By contrast, EVs were under discharging during the peak demand period. Fig. 11 shows the economic dispatch of the four power generation units in the Scenario #3. The EV discharging energy was not shown in the area plot but it acted as a negative load similar to the solar energy. The energy consumption was 27.1 MWh. The generation cost was \$1098. The average generation cost was \$40.1/MWh.

3.5. Scenario #4: V2G and solar energy penetration with 80% EVs penetration

In Scenario #4, to further investigate the flexibility of the UC model with V2G (solar and EV penetration), we increased the EV penetration to 80%. Half of the EVs were charged with 3.3 kW chargers, and the rest of the EVs were with 9.6 kW chargers.

Fig. 12 shows the load profiles of uncontrolled EV charging and EV charging and discharging curve with V2G. The blue line represents the load profile

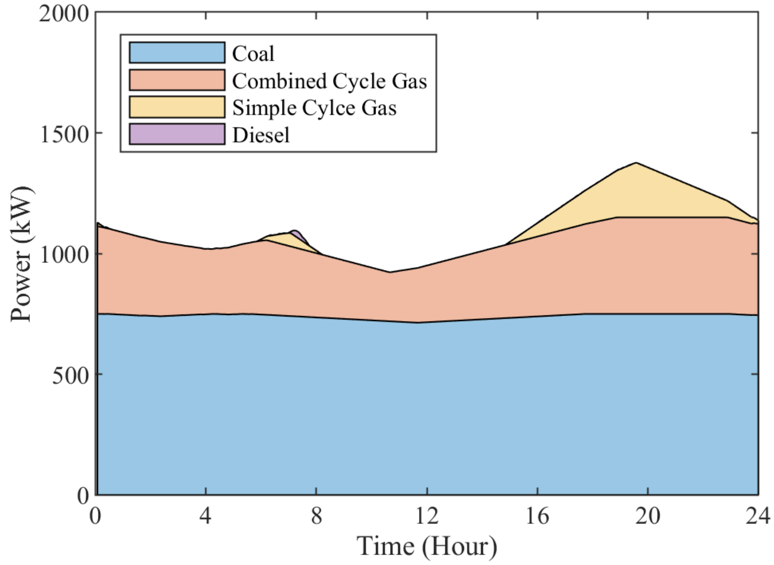

Figure 11: Power generation of different units in Scenario #3

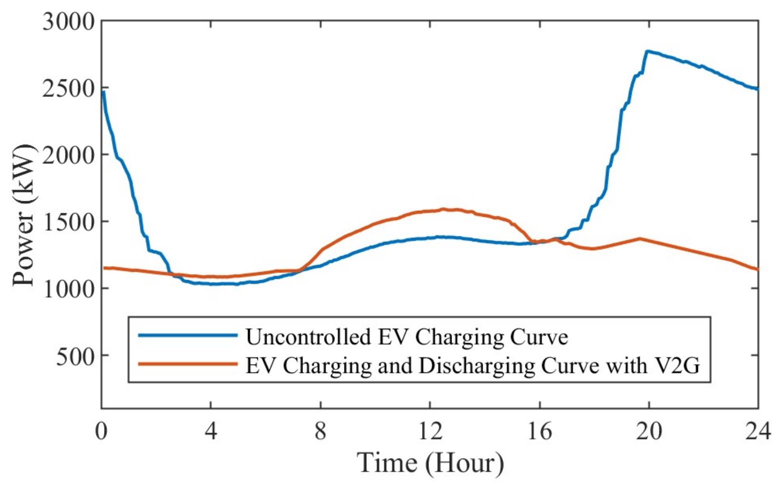

Figure 12: Uncontrolled EV charging curve and EV charging and discharging curve with V2G in Scenario #4

Table 4: Major observations in three SubScenarios of Scenario #2

#	Peak Demand kW	Load Variance kW	Max Ramping kWh/5-mins
#1	1478.1	22237.0	13.9
#2A	1741.7 (18% ↑)	42939.0 (98% ↑)	67.3 (384% ↑)
#2B	1477.4 (0%)	37529.0 (69% ↑)	29.1 (109% ↑)
#2C	1741.0 (18% ↑)	82699.0 (272% ↑)	67.4 (384% ↑)

with the uncontrolled EV charging, and the red line shows the EV charging and discharging curve with the V2G application. With uncontrolled EV charging, the peak demand and load profile variance were 2767 kW and 333990 kW, respectively. The proposed UC model with V2G reduced the peak demand by 43% to 1590 kW. It also reduced the load profile variance by 92% to 26872 kW.

4. Discussion

In this study, we have developed a V2G model and a machine learning model for solar energy prediction. We also develop a UC model that incorporates the V2G and solar energy prediction model. In the UC model, EV discharging is used as power generation, and EV charging is used as a flexible demand in DR. The predicted solar energy is considered a negative load. Experiments are designed in four scenarios to evaluate the proposed models. For a demonstration purpose, we only considered small scale power generation units, and a small number of EVs, and small scale solar energy generation. However, the proposed model is readily to be scaled up.

Table 4 summarizes the simulation results in Scenario #2. The results show that uncontrolled EV charging and solar energy can negatively impact the power system. For example, uncontrolled EV charging can increase the peak demand by 18%, if 30% of householders have EVs. To meet the increased peak demand, utilities may need to build new power plants, which requires significant investment. Solar energy can also negatively impact the power system because solar energy is not economically dispatchable and intermittent. For instance, if 20% of householders install solar panels, solar power

Table 5: Major observations in Scenario #2C and #3

#	Peak Demand kW	Load Variance kW	Max Ramping kWh/5-mins	AGC $/MWh
#2C	1741.0	82699.0	67.4	54.9
#3	1376.6 (21% ↓)	16808.0 (80% ↓)	14.1 (79% ↓)	40.1 (27% ↓)

AGC: Average Generation Cost.

can increase the load ramping rate by 109%. To meet the higher ramping load, less efficient power generators must be used, e.g., simple-cycle gas turbines or diesel generators. The usage of inefficient generators will produce more greenhouse gases and decrease the value of solar energy. Furthermore, as shown in Scenario #2C the negative impact can be superimposed with both EVs and solar energy penetration. As the current solar power generation cost is not viable comparing with conventional generators, it is not fair to compare the total generation cost between Scenario #1 and #2. We therefore do not compare the generation cost between Scenario #1 and #2.

Table 5 summarized the simulation results of Scenario #2C and #3. As can be seen, the proposed method can mitigate the negative impact of solar and uncontrolled EV penetration. Furthermore, the proposed model can incorporate V2G applications to reduce peak demand, flatten load profile, reduce generation cost, and improve energy efficiency. Specifically, the peak demand is reduced by 21%. The load variance and load ramping are decreased by 80% and 79%, respectively. Furthermore, the average generation cost is reduced by 27%. Furthermore, in the case of 80% of EV penetration, the proposed UC model with V2G reduced the peak demand and load profile variance by 43% and 92%, respectively, compared with uncontrolled EV charging. The improvement can avoid new infrastructure investment because of the reduced peak demand. Renewable energy integration and EV incorporation can also reduce greenhouse gas emissions.

5. Conclusion

The penetration of DERs poses significant challenges to power system operation. However, proper management of them can also provide benefits. To tackle the challenges and reveal the benefits, we have developed a V2G model and a solar energy prediction model. We also developed a UC model that incorporates the V2G and solar energy prediction models. Simulation results showed that uncontrolled EV charging and solar energy could negatively impact the power systems. For example, if 30% of the households have EVs and 20% of households install solar panels, the peak demand and ramping rate of the load profile would be increased by 18% and 384%, respectively. It may require building new power plants to meet the increased peak demand and using less efficient power plants to meet the increased load variation. The proposed UC model could economically dispatch EV discharging and use EV charging as a flexible demand to mitigate the negative impact and improve energy efficiency. For instance, the peak demand, ramping rate of the load profile, and average generation cost were reduced by 21%, 79%, and 27%. The proposed models can be used to quantitatively evaluate the impact of EVs and solar energy on the power systems with different penetration levels. Through the evaluation, grid operators can visualize the impact and prepare for the penetration based on their situation. The proposed UC and V2G models can also efficiently and economically integrate EVs and solar energy into power systems. Specifically, the proposed models can reduce generation costs, delay infrastructure investments, and reduce greenhouse gas emissions.

Acknowledgment

The authors would like to thank Mitacs and the University of Regina for providing funding for this study. The majority of this paper is reproduced from the M.A.Sc. thesis of Usman Munawar under the supervision of Zhanle Wang [49].

References

[1] X. Fang, S. Misra, G. Xue, D. Yang, Smart grid—the new and improved power grid: A survey, IEEE Commun. Surveys Tuts. 14 (2011) 944–980,.

[2] IESO, Structural Options for Ontario's Electricity System in a High-DER Future: Potential Implications for Reliability, Affordability, Competition and Consumer Choice, Report, Energy Transformation Network of Ontario, 2019. URL: http://www.ieso.ca/en/Learn/Ontario-Power-System/A-Smarter-Grid/Distributed-Energy-Resources.

[3] H. Wang, Z. Lei, X. Zhang, B. Zhou, J. Peng, A review of deep learning for renewable energy forecasting, Energy Conversion and Management 198 (2019) 111799.

[4] H. Jahangir, H. Tayarani, S. S. Gougheri, M. A. Golkar, A. Ahmadian, A. Elkamel, Deep learning-based forecasting approach in smart grids with micro-clustering and bi-directional lstm network, IEEE Transactions on Industrial Electronics (2020).

[5] U. Munawar, Z. Wang, A framework of using machine learning approaches for short-term solar power forecasting, Journal of Electrical Engineering & Technology 15 (2020) 561–569.

[6] P. H. Tiemann, A. Bensmann, V. Stuke, R. Hanke-Rauschenbach, Electrical energy storage for industrial grid fee reduction–a large scale analysis, Energy Conversion and Management 208 (2020) 112539.

[7] E. Bullich-Massagué, F.-J. Cifuentes-García, I. Glenny-Crende, M. Cheah-Mañé, M. Aragüés-Peñalba, F. Díaz-González, O. Gomis-Bellmunt, A review of energy storage technologies for large scale photovoltaic power plants, Applied Energy 274 (2020) 115213.

[8] K. Ginigeme, Z. Wang, Distributed optimal vehicle-to-grid approaches with consideration of battery degradation cost under real-time pricing, IEEE Access 8 (2020) 5225–5235.

[9] Z. Wang, R. Paranjape, Optimal residential demand response for multiple heterogeneous homes with real-time price prediction in a multiagent framework, IEEE transactions on smart grid 8 (2017) 1173–1184.

[10] N. Xu, C. Chung, Well-being analysis of generating systems considering electric vehicle charging, IEEE Transactions on Power Systems 29 (2014) 2311–2320.

[11] V. C. Onishi, C. H. Antunes, J. P. F. Trovão, Optimal energy and reserve market management in renewable microgrid-pevs parking lot systems: V2g, demand response and sustainability costs, Energies 13 (2020) 1884.

[12] M. Emmanuel, K. Doubleday, B. Cakir, M. Marković, B.-M. Hodge, A review of power system planning and operational models for flexibility

assessment in high solar energy penetration scenarios, Solar Energy 210 (2020) 169–180.

[13] Y. K. Semero, J. Zhang, D. Zheng, Optimal energy management strategy in microgrids with mixed energy resources and energy storage system, IET Cyber-Physical Systems: Theory & Applications 5 (2020) 80–84.

[14] E. Du, N. Zhang, B.-M. Hodge, Q. Wang, Z. Lu, C. Kang, B. Kroposki, Q. Xia, Operation of a high renewable penetrated power system with csp plants: A look-ahead stochastic unit commitment model, IEEE Transactions on Power Systems 34 (2018) 140–151.

[15] Y.-Y. Hong, G. F. D. Apolinario, Uncertainty in unit commitment in power systems: A review of models, methods, and applications, Energies 14 (2021) 6658.

[16] M. H. Imani, K. Yousefpour, M. J. Ghadi, M. T. Andani, Simultaneous presence of wind farm and v2g in security constrained unit commitment problem considering uncertainty of wind generation, in: 2018 IEEE Texas power and energy conference (TPEC), IEEE, 2018, pp. 1–6.

[17] Y. Xu, T. Ding, Q. Ming, P. Du, Adaptive dynamic programming based gas-power network constrained unit commitment to accommodate renewable energy with combined-cycle units, IEEE Transactions on Sustainable Energy (2019).

[18] S. Maghsudlu, S. Mohammadi, Optimal scheduled unit commitment considering suitable power of electric vehicle and photovoltaic uncertainty, Journal of Renewable and Sustainable Energy 10 (2018) 043705.

[19] S. Habib, M. Kamran, U. Rashid, Impact analysis of vehicle-to-grid technology and charging strategies of electric vehicles on distribution networks–a review, J. Power Sources 277 (2015) 205–214,.

[20] Z. Liu, D. Wang, H. Jia, N. Djilali, W. Zhang, Aggregation and bidirectional charging power control of plug-in hybrid electric vehicles: Generation system adequacy analysis, IEEE Trans. Sustain. Energy 6 (2014) 325–335,.

[21] I. Pavić, T. Capuder, I. Kuzle, Value of flexible electric vehicles in providing spinning reserve services, Applied Energy 157 (2015) 60–74.

[22] C. Ji, Q. Yang, N. Ning, Y. Liu, L. Lyu, Mitigating downward reserve deficiency of power system via coordinating ev demand response at valley period, IEEE Access 8 (2020) 112368–112378.

[23] A. Ahmadi, A. E. Nezhad, P. Siano, B. Hredzak, S. Saha, Information-gap decision theory for robust security-constrained unit commitment of joint renewable energy and gridable vehicles, IEEE Transactions on Industrial Informatics 16 (2019) 3064–3075.

[24] V. Vita, P. Koumides, Electric vehicles and distribution networks: Analysis on vehicle to grid and renewable energy sources integration, in: 2019 11th Electrical Engineering Faculty Conference (BulEF), IEEE, 2019, pp. 1–4.

[25] V. Vita, C. Christodoulou, I. Zafeiropoulos, I. Gonos, M. Asprou, E. Kyriakides, Evaluating the flexibility benefits of smart grid innovations in transmission networks, Applied Sciences 11 (2021) 10692.

[26] H. Q. Truong, C. Jeenanunta, Fuzzy mixed integer linear programming model for national level monthly unit commitment underprice-based uncertainty: a case study in thailand, Electric Power Systems Research 209 (2022) 107963.

[27] M. Nasir, A. R. Jordehi, M. Tostado-Veliz, V. S. Tabar, S. A. Mansouri, F. Jurado, Operation of energy hubs with storage systems, solar, wind and biomass units connected to demand response aggregators, Sustainable Cities and Society (2022) 103974.

[28] T. Logenthiran, D. Srinivasan, A. Khambadkone, H. Aung, Multi-agent system (mas) for short-term generation scheduling of a microgrid, in: 2010 ieee international conference on sustainable energy technologies (icset),IEEE, 2010, p. 1–6.

[29] I. Farhat, Economic and economic-emission operation of all-thermal and hydro-thermal power generation systems using bacterial foraging optimization, 2012.

[30] P.-H. Chen, Two-level hierarchical approach to unit commitment using expert system and elite pso, IEEE Trans. Power Syst. 27 (2011) 780–789,.

[31] T. Ji, X. Ye, M. Li, Q. Wu, X. Yang, Operating mechanism for profit improvement of a smart microgrid based on dynamic demand response, IET Smart Grid 2 (2019) 364–370.

[32] M. Nemati, M. Braun, S. Tenbohlen, Optimization of unit commitment and economic dispatch in microgrids based on genetic algorithm and mixed integer linear programming, Appl. Energy 210 (2018) 944–963.

[33] R. El-Sehiemy, M. El-Hosseini, A. Hassanien, Multiobjective real-coded genetic algorithm for economic/environmental dispatch problem, STUD INFORM CONTROL 22 (2013) 113–122.

[34] A. Parisio, E. Rikos, L. Glielmo, A model predictive control approach to microgrid operation optimization, IEEE Trans. Control Syst. Technol. 22 (2014) 1813–1827,.

[35] M. Carrión, J. Arroyo, A computationally efficient mixed-integer linear formulation for the thermal unit commitment problem, IEEE Trans. Power Syst. 21 (2006) 1371–1378,.

[36] X. Wu, X. Wang, Z. Bie, Optimal generation scheduling of a microgrid, in: 2012 3rd IEEE PES Innovative Smart Grid Technologies Europe (ISGT Europe), IEEE, 2012, p. 1–7.

[37] M. Amini, R. Jaddivada, S. Mishra, O. Karabasoglu, Distributed security constrained economic dispatch, in: 2015 IEEE Innovative Smart Grid Technologies-Asia (ISGT ASIA), IEEE, 2015, p. 1–6.

[38] K. Boroojeni, M. Amini, S. Iyengar, M. Rahmani, P. Pardalos, An economic dispatch algorithm for congestion management of smart power networks, Energy Syst. 8 (2017) 643–667.

[39] I. Pavić, T. Capuder, I. Kuzle, A comprehensive approach for maximizing flexibility benefits of electric vehicles, IEEE Systems Journal 12 (2017) 2882–2893.

[40] A. Soares, C. Antunes, C. Oliveira, A. Gomes, A multi-objective genetic approach to domestic load scheduling in an energy management system, Energy J. 77 (2014) 144–152.

[41] N. Hackathon, Solar radiation prediction, 2017.

[42] arcadia, Calculating your kilowatt hour usage at home?, 2022. URL: https://blog.arcadia.com/calculating-your-kilowatt-hour-usage-at-home/, accessed.

[43] S. Wong, Summary report on canadian residential demand response and ancillary service market opportunities, Natural Resources Canada (2019). URL: https://www.nrcan.gc.ca/energy/offices-labs/canmet/publications/smart-grid/17735.

[44] EIA, How much electricity does an american home use?, 2022. URL: eia.gov/tools/faqs/faq.php?id=97&t=3, accessed.

[45] P.J.M., 2020. URL: https://www.pjm.com/markets-and-operatio, accessed on:.

[46] C.V.X., Matlab software for disciplined convex programming, version 2.0 beta, 2013-09. URL: http://cvxr.com/cvx, available:.

[47] V. Vidyasagar), S. Boyd, H. Kimura (Eds.), Graph implementations for nonsmooth convex programs, Recent Advances in Learning and Control (a tribute to M, Lecture Notes in Control and Information Sciences, Springer, 2008. URL: http://stanford.edu/~boyd/graph_dcp.html.

[48] L. Gurobi Optimization, Gurobi optimizer reference manual, 2020. URL: http://www.gurobi.com.

[49] U. Munawar, Coordinated integration of distributed energy resources in unit commitment, Ph.D. thesis, The University of Regina (Canada), 2021.